Applied Surface Science 263 (2012) 410–415

Contents lists available at SciVerse ScienceDirect

Applied Surface Science

journal homepage: www.elsevier.com/locate/apsusc

Site-controlled synthesis and mechanism of three-dimensional Mo_2S_3 flowers

Yu Zhong, Yong Zhang, Gaixia Zhang, Ruying Li, Xueliang Sun*

Department of Mechanical and Materials Engineering, University of Western Ontario, London, Ontario, Canada N6G 5B9

ARTICLE INFO

Article history:
Received 10 August 2012
Received in revised form
12 September 2012
Accepted 15 September 2012
Available online 23 September 2012

Keywords:
Mo_2S_3 flowers
Three-dimensional
CVD
Au particles

ABSTRACT

High-density three-dimensional Mo_2S_3 flowers have been facilely synthesized with controlled sites by introducing gold particles as the nucleation sites in a chemical vapor deposition process. The whole size of each flower is in micro scale while individual petal has extremely small thickness of around 10 nm. The role of gold particles and precursor concentration in the growth has been carefully investigated. Without gold particles, dense nanopetals were not able to be obtained unless in a highly concentrated sulfur atmosphere. With Au particles, dense products were steadily achieved in a wide precursor concentration range with S:MoO_3 molar ratio from 1:5 to 5:1. The morphology and structure of the as-synthesized nanostructures were characterized using field emission scanning electron microscopy (FE-SEM) and high-resolution transmission electron microscopy (HRTEM). The growth mechanism was proposed in which gold particles acted as the initial nucleation sites fixing the nucleation position of the flowers following vapor–solid growth mechanism.

1. Introduction

Nanomaterials have attracted intensive research interest in the past decade for their novel structure and potential applications [1–4]. Recently, nanostructured metal chalcogenides have received particular attention. Among various metal chalcogenide nanostructures, nanostructured MoS_2 have been extensively investigated due to their applications for electrode materials [5], electrochemical hydrogen storage [6] and optoelectronics [7]. Up to now, nanostructured MoS_2 with different dimensions have been prepared including nanowires [8], nanotubes [9,10], flowers [11,12] and nanospheres [13] by various methods, such as chemical vapor deposition (CVD) [14], hydrothermal synthesis [15,16], template method [17,18] and sulfurization of MoO_2 [11]. The comprehensive investigation of MoS_2 has also stimulated the research on the trivalent molybdenum sulfide, Mo_2S_3 [19–21]. Mo_2S_3 nanostructure can be either prepared by a solid–gas reaction between MoO_3/Al_2O_3 support material and H_2S [20], or converted by MoS_2 via a certain treatment [22]. In addition, for most practical applications, it is an important prerequisite to assemble nanoscale building blocks directly on a suitable conductive substrate. However, controlled synthesis of uniform Mo_2S_3 flowers with stably high density and controllable growth sites on an appropriate conductive substrate still remains a challenge.

In this work, we describe a facile way to synthesize uniform Mo_2S_3 flowers with steadily high density and controllable growth sites on conductive carbon paper substrate by introducing gold particles to trigger the growth in a CVD process. Without gold particles, nanopetals could be observed under a very dense S concentration. While gold was introduced, dense products with flower-like morphology could be readily obtained in a wide range of S:MoO_3 molar ratio and the flowers preferably grew on the gold particles. The effects of S and Au on the growth of nanostructure were investigated.

2. Materials and methods

The nanostructures were prepared via CVD method. The synthesis was performed in a quartz tube which was mounted in an electric furnace. S (Aldrich 99.98%) and MoO_3 (Aldrich 99.5%) powders as the starting materials were loaded in ceramic boats, respectively, with the molar ratio varying from 1:5 to 5:1. The MoO_3 powders were placed at the center of the quartz tube, while the S powders were put at the entrance of the furnace, upstream of an Ar flow which acted as carrier gas. A commercial carbon paper (E-TEK) used as the substrate was put near the ceramic boat containing MoO_3 powders at the down stream of the Ar flow. Two kinds of carbon paper were used: one was plain carbon paper without any pre-treatment; the other one was pre-treated by depositing a very thin Au film on the surface. The quartz tube was purged by Ar flow prior to the synthesis. Then the furnace was heated up to the reaction temperature (810 °C), and kept for 2 h to make the starting materials react completely. Finally the furnace was cooled down to the room temperature.

The products collected from the surface of the carbon paper were investigated by field emission scanning electron microscopy

---

* Corresponding author. Tel.: +1 519 661 2111x87759.
E-mail address: xsun@eng.uwo.ca (X. Sun).

0169-4332/$ – see front matter © 2012 Elsevier B.V. All rights reserved.
http://dx.doi.org/10.1016/j.apsusc.2012.09.070

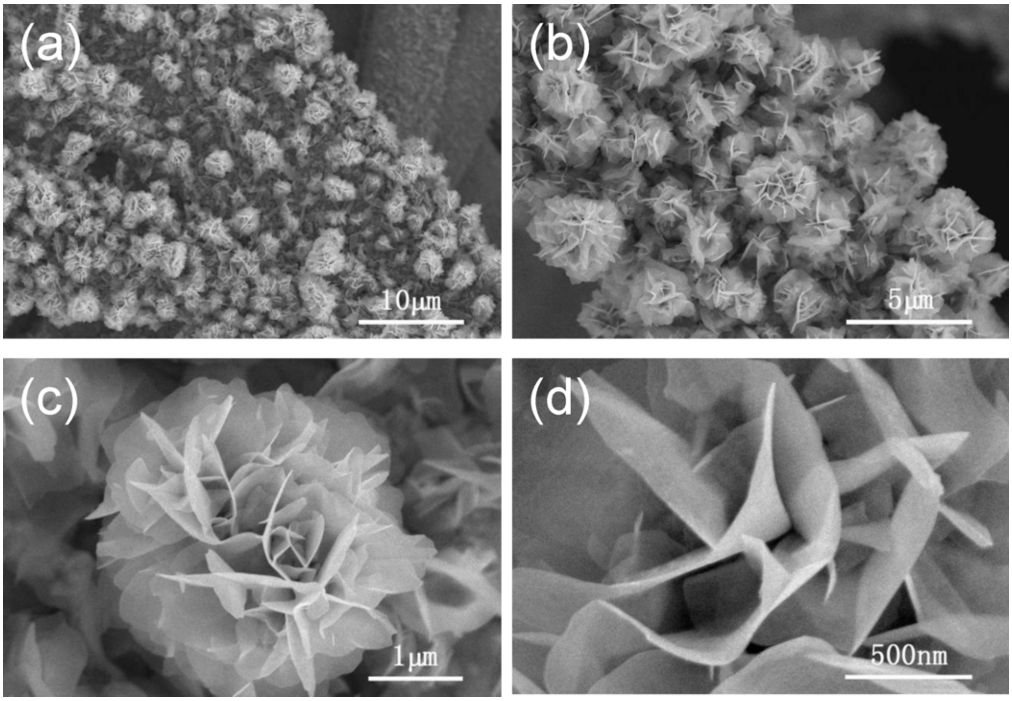

Fig. 1. SEM images of as-synthesized nanoflowers with Au particles with S/MoO_3 molar ratio of 1:1.

(FE-SEM, Hitachi 4800S) and high-resolution transmission electron microscopy (HRTEM, JEOL 2010 FEG).

3. Results and discussion

Fig. 1 shows SEM images of the typical Mo_2S_3 flowers synthesized with S:MoO_3 molar ratio of 1:1 in the starting materials on carbon paper with Au particles. Dense products were observed on the carbon fiber (Fig. 1a). The products feature three-dimensional flower-like morphology (Fig. 1b). The entire diameter of the nanoflowers is from 1.9 to 3.6 μm. Each flower consists of tens to hundreds of pieces of nanopetals (Fig. 1c). The nanopetals have very smooth surface and sharp edge, and are slightly curved (Fig. 1d). The nanopetals are from 500 nm to 2.3 μm in width and have extremely thin thickness of around 10 nm.

HRTEM images are shown in Fig. 2. Fig. 2a depicts that the nanopetals are a little curved and quite thin, which is consistent with SEM results. The HRTEM image (Fig. 2b) and fast Fourier transformation (FFT) diffraction pattern (inset of Fig. 2b) are from the same individual nanopetal and reveal the high crystallinity of the petal. The interplanar distance is measured of 0.24 nm and belongs to the plane $(\bar{1}\,1\,2)$ of Mo_2S_3. The FFT diffraction pattern can be indexed as $(\bar{2}\,0\,1)$, $(\bar{1}\,1\,2)$ and $(1\,1\,1)$ crystal planes of monoclinic Mo_2S_3 (JCPDS card no.: 81-2031).

To investigate the effects of precursor concentration and gold particles on the growth of the Mo_2S_3 nanopetals, the growth without and with gold particles was carried out using different molar ratio of S:MoO_3 varied from 1:5 to 5:1 in the starting materials. The results of the growth without gold particles are shown in Fig. 3. With quite a small S:MoO_3 molar ratio of 1:5, many tiny particles and quite a few nanopetals were observed on the surface of carbon substrate (Fig. 3a and b). The size of nanopetals is from 450 nm to 1.5 μm in width and about 40 nm in thickness. By increasing the S:MoO_3 ratio to 1:1, bundles of small flowers appeared (Fig. 3c). The small flowers compose of very tiny petals with sharp edge and approximately 3 μm in the width (Fig. 3d). However, the amount of bundles of flowers is quite small, and most of the surface of the substrate is exposed. Keeping increasing the S:MoO_3 ratio to 5:1, the carbon substrate was completely covered by dense nanopetals (Fig. 3e). These nanopetals with sharp edge and thin thickness around several nanometers are quite dense and close-packed. The size of nanopetal is in a wide range from 500 nm to 3.2 μm in width

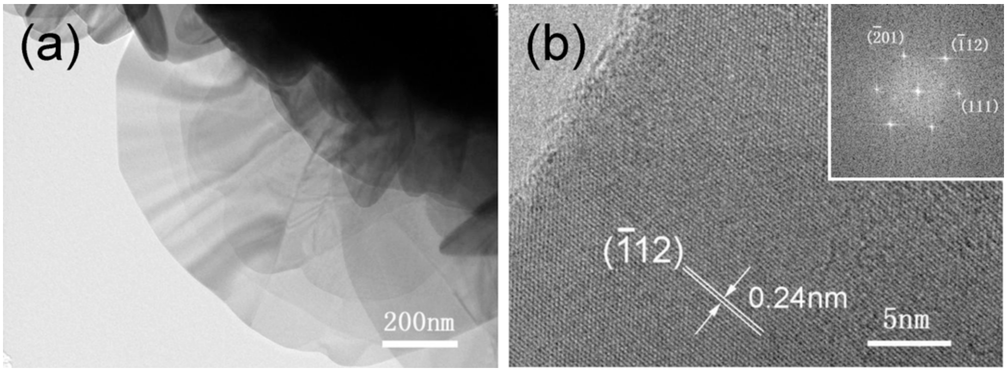

Fig. 2. HRTEM images of nanopetals synthesized with Au particles with S/MoO_3 molar ratio of 1:1. (a) TEM image of morphology of individual nanopetal; (b) HRTEM image shows the lattice image of nanopetal, inset showing the FFT diffraction pattern.

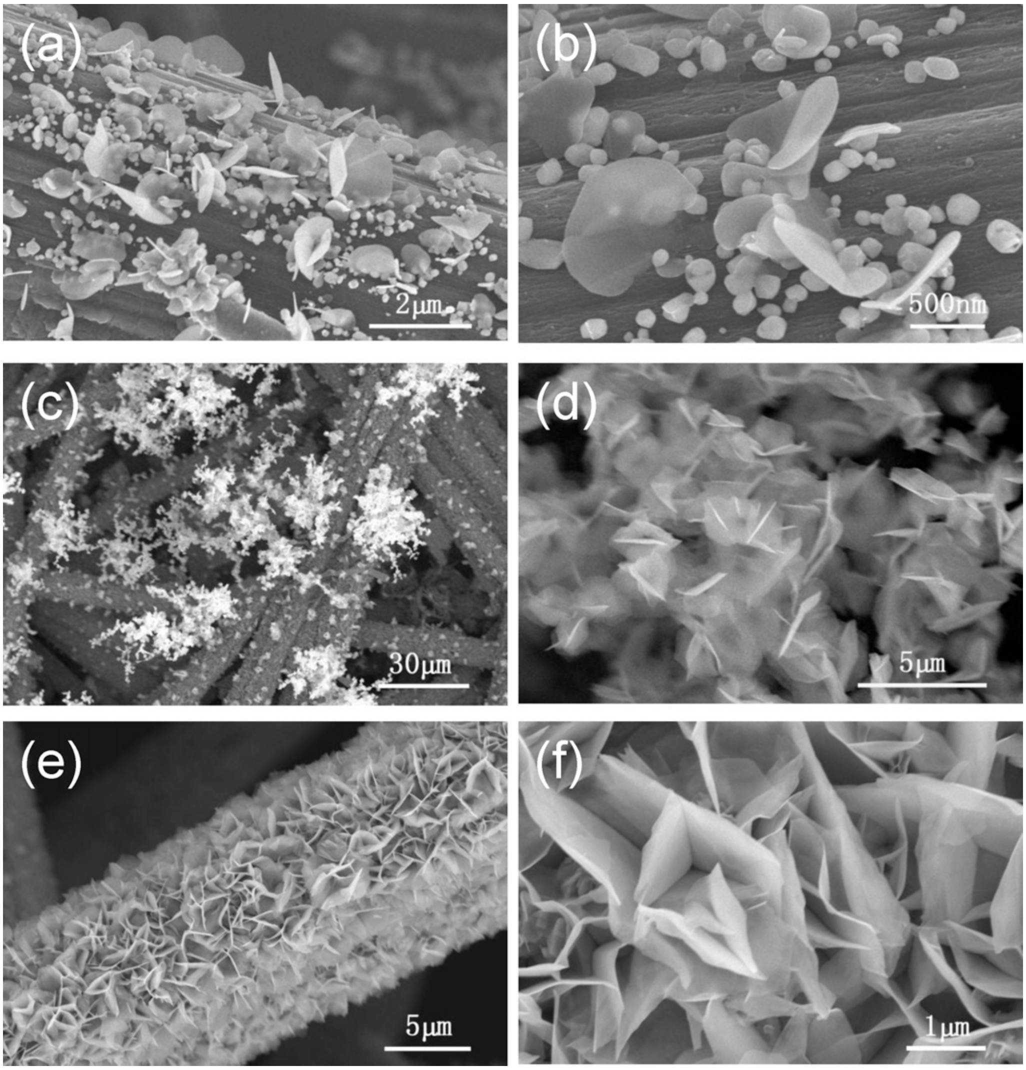

Fig. 3. SEM images of the as-synthesized nanostructures without Au particles. (a) and (b) for S/MoO_3 molar ratio of 1:5; (c) and (d) for S/MoO_3 molar ratio of 1:1; (e) and (f) for S/MoO_3 molar ratio of 5:1.

(Fig. 3f). The above results indicate that the growth of nanostructure is affected by the concentration of S vapor. Concentrated S atmosphere can induce the growth of dense nanopetals and increasing the concentration of S could enhance the growth of the nanostructures.

On the other hand, aiming at controlled nucleation and growth of the flowers, a thin Au film could be introduced into the system since Au is a very popular catalyst in the growth of nanostructures [23–29]. A very thin Au film was deposited on the surface of carbon paper and all other experimental parameters were kept the same. SEM observation shows that the Au film is actually exhibited as well-dispersed Au particles with the diameter around 12–26 nm (Supplementary Fig. S1).

Fig. 4 shows the SEM images of nanostructures synthesized in the presence of Au at different S:MoO_3 molar ratio from 1:5 to 5:1. With the Au particles, though at relatively low concentration of S (S:MoO_3 molar ratio of 1:5), quite a big amount of nanopetals grew on the substrate shown in Fig. 4a. The nanopetals are very big from 600 nm to 4 μm in width and around 10 nm in thickness, and show sharp edge and smooth surface (Fig. 4b). Increasing the S:MoO_3 ratio to 1:1, dense nanopetals were close-packed and formed many flowers on the surface of carbon substrate (Fig. 4c). The size of these flowers is from 1.9 to 3.6 μm. Each flower composes of many petals and presents a three-dimensional morphology with an open structure which provides a huge specific surface (Fig. 4d). All the petals of the flowers have an extremely thin thickness, sharp edge and very smooth and clean surface. However, if the S:MoO_3 ratio was further increased to 5:1, the growth of nanostructure was influenced by the dense S atmosphere. The products still remain the nanopetal shape with the similar size but low density, and are not close-packed (Fig. 4e). Some of the petals are bent and not clean at the surface. There are many very tiny pieces of cracks as impurities decorated at the surface of nanopetals (Fig. 4f). Many particles which are another source of impurities are also observed at the roots and among the nanopetals.

By comparing the results with and without Au particles, the effect of Au is revealed. Without Au, dense nanopetals are only obtained in a very dense S atmosphere (S:MoO_3 ratio of 5:1). However, after introducing Au into the system, dense nanopetals and flowers can be steadily generated in a wide range of S:MoO_3 ratio from 1:5 to 5:1, which indicates that Au plays a very important role in the growth of the nanostructure. To investigate the effect of Au on the growth of nanostructure, the growth mechanism has been studied and proposed.

Scrutiny of the product morphology by SEM and TEM indicates that no melting behavior of the gold particles was observed, implying that the growth followed vapor–solid (VS) mechanism [30] instead of the so-called vapor–liquid–solid (VLS) mode [26,27]. The

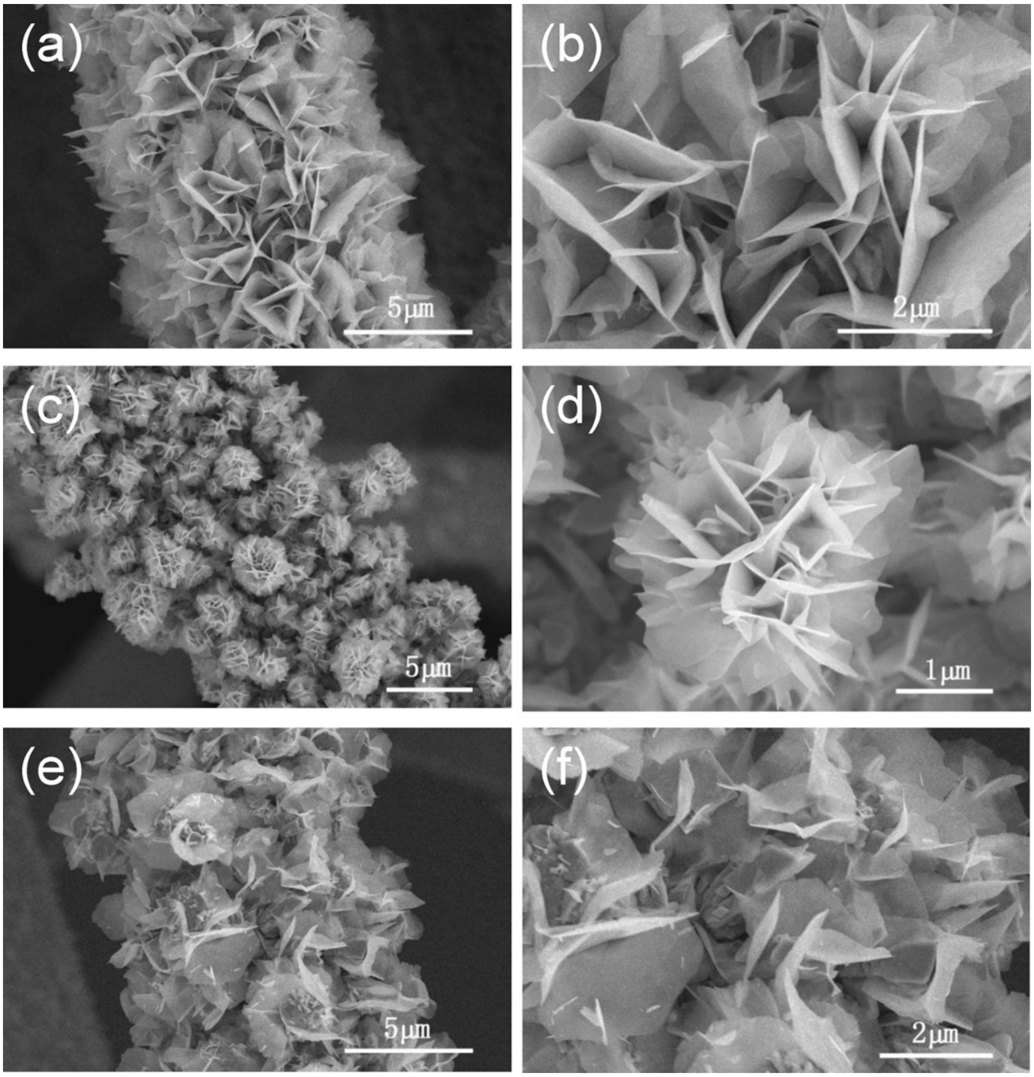

Fig. 4. SEM images of the as-synthesized nanostructures with Au particles. (a) and (b) for S/MoO_3 molar ratio of 1:5; (c) and (d) for S/MoO_3 molar ratio of 1:1; (e) and (f) for S/MoO_3 molar ratio of 5:1.

growth mechanisms of the nanostructure with and without Au are similar, but the presence of Au makes it easier to trigger the growth.

Without the assistance of Au on the carbon substrate, at the beginning of the reaction, S (melting point: 115 °C) and MoO_3 (melting point: 795 °C) are evaporated and react in the vapor phase (Fig. 5a). MoO_3 is sulfided into Mo_2S_3 and transported to the carbon substrate by Ar carrier gas (Fig. 5b). The Mo_2S_3 precursors deposit on the surface of the plain carbon substrate and nucleate randomly depending on the surface conditions of the substrate. Then the continuous deposition of precursors happens at the surface of initial nuclei and the nuclei grow into big nanopetals and flowers following the VS mode [30]. In a VS mode, the amount of initial nuclei determines the growth density of nanostructures: more initial nuclei which provide more growth sites will result in denser products. However, the dense products are only obtained in highly concentrated S atmosphere (S:MoO_3 ratio of 5:1) which leads to the complete reaction between the starting materials and provides enough Mo_2S_3 precursors for the growth. That indicates without the assistance of Au the S concentration plays an important role in the nucleation and growth of the nanostructures. In the concentrated S atmosphere, high supersaturation of reactive precursors facilitates the formation of dense nuclei (Fig. 5f). The nuclei finally grow into big nanopetals and flowers (Fig. 5g and h). While at relatively low S concentration, nucleation only randomly occurs at some inhomogeneous sites of the bare carbon substrate which merely generates sparse nuclei (Fig. 5c and Supplementary Fig. S2), leading to a low density of final products (Fig. 5d).

On the other hand, when a very thin Au film is introduced, a large amount of Au particles can form on the surface of the substrate (Fig. 5e and Supplementary Fig. S1). These Au particles act as the initial growth sites at which the precursors are much easier to deposit at various S:MoO_3 ratios (Fig. 5f and Supplementary Fig. S3). Usually Au can be used to grow some novel nanostructures, like nanowires, in a VLS mode [26,27]. In the typical VLS mode, firstly Au particles absorb and alloy with the gaseous starting materials. When the Au particles are liquefied and supersaturated with the materials, the materials will precipitate and form nanostructures [27]. However, it is quite difficult to yield Au–S alloy due to the high volatilization of S and no melting behavior of the gold particles was observed as mentioned above [31]. Thus the growth of Mo_2S_3 nanopetals and flowers with Au particles is not a VLS process. We think Au particles here provide a low surface–energy interface and act as preferential sites for adsorbing Mo and S gaseous precursors, thereby facilitating the reaction of the starting materials and the nucleation and growth of Mo_2S_3 nanostructures [32]. Due to layered structure of Mo_2S_3, the dangling bonds on the edges of the initial sulfide nuclei can incorporate atoms directly from the gaseous precursors while the surface of the petals keep smooth and unreactive, which favors

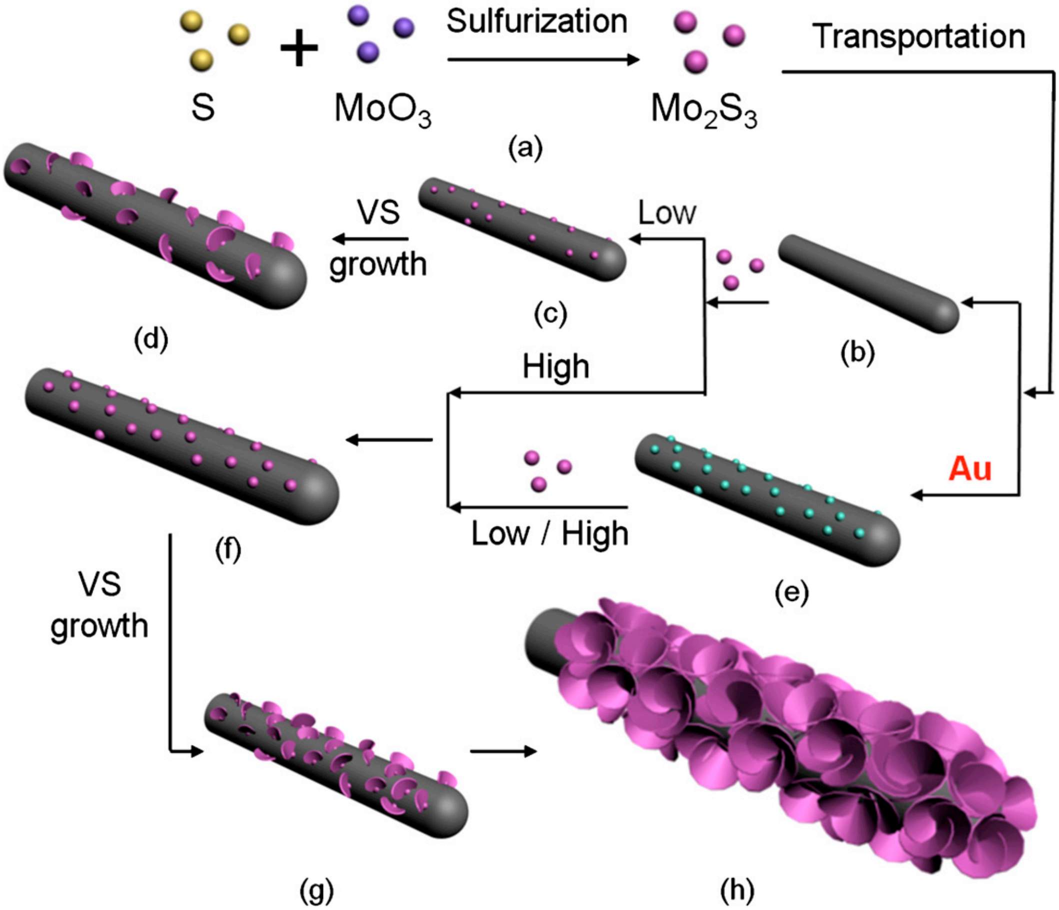

Fig. 5. A schematic growth mechanism of nanopetals and flowers with and without Au particles. (a) sulfurization of MoO_3 by S; (b) Deposition of Mo_2S_3 on plain carbon substrate (c) less Mo_2S_3 nuclei at low S concentration; (d) less and small nanopetals growing on plain carbon substrate at low S concentration; (e) carbon substrate with Au particles forming at the surface; (f) uniform and dense Mo_2S_3 nuclei forming at the carbon substrate; (g) and (h) Mo_2S_3 nuclei growing into dense nanopetals and flowers.

lateral growth of the nanopetals and the architecture of flowers are finally obtained (Fig. 5g, h and Supplementary Fig. S4). Owing to the assistance of Au particles, the precursors are easily collected for the following nucleation in a wide S concentration range, and site-controlled growth of the flowers is realized based on VS growth mechanism (Fig. 5e–h).

4. Conclusions

Site-controlled growth of three-dimensional Mo_2S_3 flowers was realized with the assistance of Au particles in optimal concentrated S atmosphere in a CVD process. The effects of S concentration and Au particles were investigated. Without the assistance of Au particles, only high concentration S atmosphere can lead to the enhanced growth of the nanostructures. In the presence of Au particles, the growth of nanostructures is very easily triggered even in a wide range of S:MoO_3 molar ratio from 1:5 to 5:1. At the optimal S:MoO_3 ratio of 1:1, a big amount of flowers were obtained on the surface of the carbon substrate. The stable synthesis of high-density three-dimensional Mo_2S_3 flowers makes it possible for the applications in producing different nanodevices such as electrode materials for lithium-ion battery and field emission applications.

Acknowledgements

This research was supported by National Science and Engineering Research Council (NSERC), Canada Research Chair (CRC) program, Canadian Foundation for Innovation (CFI), and the University of Western Ontario. The authors also appreciate the help from Mr. Fred Pearson at McMaster University.

Appendix A. Supplementary data

Supplementary data associated with this article can be found, in the online version, at http://dx.doi.org/10.1016/j.apsusc.2012.09.070.

References

[1] S. Iijima, Nature 354 (1991) 56.
[2] C. Liu, Y.Y. Fan, M. Liu, H.T. Cong, H.M. Cheng, M.S. Dresselhaus, Science 286 (1999) 1127.
[3] J. Kong, N.R. Franklin, C. Zhou, M.G. Chapline, S. Peng, K. Cho, H. Dai, Science 287 (2000) 622.
[4] P. Kim, C.M. Lieber, Science 286 (1999) 2148.
[5] N. Imanishi, K. Kanamura, Z. Takehara, J. Electrochem. Soc. 139 (1992) 2082.
[6] J. Chen, N. Kuriyama, H. Yuan, H.T. Takeshita, T. Sakai, J. Am. Chem. Soc. 123 (2001) 11813.
[7] A. Kis, D. Mihailovic, M. Remskar, A. Mrzel, A. Jesih, I. Piwonski, A.J. Kulik, W. Benoît, L. Forró, Adv. Mater. 15 (2003) 733.
[8] W.J. Li, E.W. Shi, J.M. Ko, Z.Z. Chen, H. Ogino, T. Fukuda, J. Cryst. Growth 250 (2003) 418.
[9] Li X.L. Li, J.P. Ge, Y.D. Li, Chem. Eur. J. 10 (2004) 6163.
[10] Y. Peng, Z. Meng, C. Zhong, J. Lu, Z. Yang, Y. Qian, Mater. Chem. Phys. 73 (2002) 327.
[11] Y.B. Li, Y. Bando, D. Golberg, Appl. Phys. Lett. 82 (2003) 1962.
[12] R. Wei, H. Yang, K. Du, W. Fu, Y. Tian, Q. Yu, S. Liu, M. Li, G. Zou, Mater. Chem. Phys. 108 (2008) 188.
[13] Y. Tian, X. Zhao, L. Shen, F. Meng, L. Tang, Y. Deng, Z. Wang, Mater. Lett. 60 (2006) 527.
[14] W.Y. Lee, T.M. Besmann, M.W. Stott, J. Mater. Res. 9 (1994) 1474.
[15] Y. Tian, Y. He, Y. Zhu, Mater. Chem. Phys. 87 (2004) 87.

[16] Y. Peng, Z. Meng, C. Zhong, J. Lu, W. Yu, Z. Yang, Y. Qian, J. Solid State Chem. 159 (2001) 170.
[17] C.M. Zelenski, P.K. Dorhout, J. Am. Chem. Soc. 120 (1998) 734.
[18] P. Santiago, J.A. Ascencio, D. Mendoza, M. Pérez-Alvarez, A. Espinosa, C. Reza-Sangermán, P. Schabes-Retchkiman, G.A. Camacho-Bragado, M. José-Yacamán, Appl. Phys. A 78 (2004) 513.
[19] F. Jellinek, Nature 192 (1961) 1065.
[20] R.C. Che, N. Bai, L.-M. Peng, Appl. Phys. Lett. 83 (2003) 3561.
[21] R.L. Fagerquist, R.D. Kirby, Phys. Rev. B 38 (1988) 3973.
[22] R.K. Tiwari, J.S. Yang, M. Saeys, C. Joachim, Surf. Sci. 602 (2008) 2628.
[23] F. Yu, D. Tang, K. Hai, Z. Luo, Y. Chen, X. He, Y. Peng, H. Yuan, D. Zhao, Y. Yang, J. Cryst. Growth 312 (2010) 220.
[24] S. Budak, G.X. Miao, M. Ozdemir, K.B. Chetry, A. Gupta, J. Cryst. Growth 291 (2006) 405.
[25] C.K. Chan, R.N. Patel, M.J. O'Connell, B.A. Korgel, Y. Cui, ACS Nano 4 (2010) 1443.
[26] C.K. Chan, X.F. Zhang, Y. Cui, Nano Lett. 8 (2008) 307.
[27] W. Yin, B. Wei, C. Hu, Chem. Phys. Lett. 471 (2009) 11.
[28] S. Park, C. Hong, J. Kang, N. Cho, C. Lee, Curr. Appl. Phys. 9 (2009) S230.
[29] L.V. Thong, N.D. Hoa, D.T.T. Le, D.T. Viet, P.D. Tam, A.T. Le, N.V. Hieu, Sens. Actuators B 146 (2010) 361.
[30] N. Wang, Y. Cai, R.Q. Zhang, Mater. Sci. Eng. Rep. 60 (2008) 1.
[31] H. Okamoto, T.B. Massalski, Bull. Alloy Phase Diagram. 6 (1985) 518.
[32] K.A. Dick, K. Deppert, T. Mårtensson, B. Mandl, L. Samuelson, W. Seifert, Nano Lett. 5 (2005) 761.